Available online at www.sciencedirect.com
SCIENCE DIRECT
Journal of Solid State Chemistry 179 (2006) 1911–1917
JOURNAL OF SOLID STATE CHEMISTRY
www.elsevier.com/locate/jssc

Rapid Communication

Syntheses, crystal structures and characterizations of $BaZn(SeO_3)_2$ and $BaZn(TeO_3)Cl_2$

Hai-Long Jiang, Mei-Ling Feng, Jiang-Gao Mao*

State Key Laboratory of Structural Chemistry, Fujian Institute of Research on the Structure of Matter, Chinese Academy of Sciences, and the Graduate School of the Chinese Academy of Sciences, Fuzhou 350002, PR China

Received 14 December 2005; received in revised form 7 February 2006; accepted 16 March 2006
Available online 24 April 2006

Abstract

Two new barium zinc selenite and tellurite, namely, $BaZn(SeO_3)_2$ and $BaZn(TeO_3)Cl_2$, have been synthesized by the solid state reaction. The structure of $BaZn(SeO_3)_2$ features double chains of $[Zn(SeO_3)_2]^{2-}$ anions composed of four- and eight-member rings which are alternatively along *a*-axis. The double chains of $[Zn_2(TeO_3)_2Cl_3]^{3-}$ anions in $BaZn(TeO_3)Cl_2$ are formed by Zn_3Te_3 rings in which each tellurite group connects with three ZnO_3Cl tetrahedra. $BaZn(SeO_3)_2$ and $BaZn(TeO_3)Cl_2$ are wide bandgap semiconductors based on optical diffuse reflectance spectrum measurements.

Keywords: Solid state reaction; Crystal structure; Selenite; Tellurite; Open framework

1. Introduction

Metal selenites and tellurites can adopt many unusual structures due to the presence of the stereochemically active lone pair [1]. The asymmetric coordination polyhedron adopted by Se(IV) or Te(IV) atom may result in non-centrosymmetric structures with consequent interesting physical properties, such as nonlinear optical second harmonic generation (SHG) [2–4]. Furthermore, transition metal Se(IV) or Te(IV) oxyhalides can be regarded as "chemical scissors" since the effective volume of the lone pair is approximately the same as the volume of an O^{2-} ion, and they are promising new low-dimensional magnets [5]. In other words, the lone pair acts as an invisible structural directing agent. A large number of transition metal selenites and tellurites have been reported. As for zinc(II) metal, the reported selenites include $ZnSeO_3$ [6], $ZnSe_2O_5$ [7], $Zn_2(SeO_3)Cl_2$ [8], $Zn_3Fe_2(SeO_3)_6$ [9] and $ZnFe_2(SeO_3)_4$ [10], and zinc Te(IV) oxides such as $ZnTeO_3$ [11], $Zn_2Te_3O_8$ [12], $Zn_2(TeO_3)Cl_2$ [13], and $CuZn(TeO_3)Cl_2$ [14] also have been reported. The alkaline earth cations may serve as bridges between zinc selenite or tellurite anionic building units to form new architectures. Furthermore, these compounds may possess new physical properties. However, reports on alkaline earth zinc selenites and tellurites are scarce [15–19]. So far such compounds structurally characterized include $SrZn(SeO_3)_2$ [15], $BaCo(SeO_3)_2$ [16], $MCu(SeO_3)_2$ (M = Sr, Ba) [17], $SrMn(SeO_3)_2$ [18] and $SrCu(TeO_3)_2$ [19].

Our exploration on new phases formed in Ba–Zn–Te(Se)–O system afforded two new compounds, namely, $BaZn(SeO_3)_2$ and $BaZn(TeO_3)Cl_2$. Herein we report their syntheses, crystal structures and characterizations.

2. Experimental

2.1. Materials and instrumentation

All chemicals except BaO were obtained from commercial sources and used without further purification. BaO was obtained by heating $BaCO_3$ at 400 °C for 12 h. IR spectrum was recorded on a Magna 750 FT–IR spectrometer photometer as a KBr pellet in the 4000–400 cm^{-1} range. Microprobe elemental analyses on Ba, Zn, Se, Te and Cl were performed on a field emission scanning electron microscope (FESEM, JSM6700F) equipped with an energy

*Corresponding author. Fax: +86 591 371 4946.
E-mail address: mjg@ms.fjirsm.ac.cn (J.-G. Mao).

0022-4596/$ - see front matter © 2006 Elsevier Inc. All rights reserved.
doi:10.1016/j.jssc.2006.03.018

dispersive X-ray spectroscope (EDS, Oxford INCA). X-ray powder diffraction (XRD) patterns (Cu$K\alpha$) were collected on an XPERT-MPD $\theta-2\theta$ diffractometer. Optical diffuse reflectance spectra were measured at room temperature with a PE Lambda 900 UV-Visible spectrophotometer. The instrument was equipped with an integrating sphere and controlled by a personal computer. The samples were ground into fine powder and pressed onto a thin glass slide holder. $BaSO_4$ plate was used as a standard (100% reflectance). The absorption spectra were calculated from reflectance spectra using the Kubelka–Munk function: $\alpha/S = (1-R)^2/2R$ [20], where α is the absorption coefficient, S is the scattering coefficient which is practically wavelength independent when the particle size is larger than 5 μm, and R is the reflectance. Thermogravimetric analyses (TGA) were carried out with a NETZSCH STA 449C unit, at a heating rate of 10 °C/min under an oxygen atmosphere.

2.2. Syntheses of $BaZn(SeO_3)_2$ and $BaZn(TeO_3)Cl_2$

Colorless needle-shaped single crystals of $BaZn(SeO_3)_2$ were initially obtained by the solid state reaction of 0.8 mmol of $BaCO_3$, 1.6 mmol of ZnO and 1.2 mmol SeO_2 in an evacuated quartz tube at 750 °C for 6 days and then cooled to 350 °C at 4 °C/h before switching off the furnace. Its chemical composition was also confirmed by microprobe elemental analyses on several single crystals (Ba:Zn:Se = 1.0:0.9:2.3). Subsequently, a pure powder sample of $BaZn(SeO_3)_2$ was prepared quantitatively by reacting a mixture of BaO, ZnO and SeO_2 in a molar ratio of 1:1:2 at 660 °C. IR data (KBr, cm^{-1}): 854 (s), 799 (vs), 720 (vs), 596 (m), 499 (s), 459 (m), 421 (w).

$BaZn(TeO_3)Cl_2$ was synthesized by high-temperature reaction of 0.6 mmol of $BaCl_2$, 0.6 mmol of ZnO and 0.6 mmol of TeO_2 by a similar method. The reaction mixture was thoroughly ground and pressed into a pellet, which was then put into an evacuated quartz tube. The quartz tube was heated at 720 °C for 6 days and then cooled to 300 °C at 4 °C/h before switching off the furnace. Colorless needle-shaped crystals of $BaZn(TeO_3)Cl_2$ were obtained as a single phase. The measured molar ratio of Ba:Zn:Te:Cl by microprobe elemental analysis is 1.0:0.9:1.0:2.1, which is in good agreement with the one determined from single crystal X-ray structural analysis. IR data (KBr, cm^{-1}): 738 (s), 687 (vs), 574 (m), 471 (w) and 418 (w).

2.3. Crystal structure determination for $BaZn(SeO_3)_2$ and $BaZn(TeO_3)Cl_2$

Single crystals of the above two compounds were mounted on glass fibers and data collections were performed on a Rigaku Mercury CCD (Mo$K\alpha$ radiation, graphite monochromator). Intensity data were collected by the narrow frame method at 293 K. The data were corrected for lorentz factor, polarization, air absorption and absorption due to variations in the path length through the detector faceplate. Absorption correction based on Multi-scan technique was also applied [21]. The space groups were determined to be $P2_1/n$ for $BaZn(SeO_3)_2$ and *Pnma* for $BaZn(TeO_3)Cl_2$ based on systematic absences as well as E-value statistics, which gave satisfactory refinements for both compounds. Both structures were solved by the direct methods and refined by full-matrix least-squares fitting on F^2 by SHELXS-97 [22]. The data collection and refinement parameters are summarized in Table 1. The atomic coordinates, selected bond lengths are listed in Tables 2 and 3, respectively.

Table 1
Crystal data and structure refinements for $BaZn(SeO_3)_2$ and $BaZn(TeO_3)Cl_2$

Formula	$BaZnSe_2O_6$	$BaZnTeO_3Cl_2$
Fw	456.63	449.21
Space group	$P2_1/n$ (No. 14)	*Pnma* (No. 62)
a (Å)	5.5375(7)	12.345(4)
b (Å)	16.429(2)	5.6458(19)
c (Å)	7.1683(9)	19.186(7)
β (°)	96.671(5)	90
V (Å^3)	647.72(14)	1337.2(8)
Z	4	8
D_{calcd} (g cm^{-3})	4.683	4.463
μ (Mo$K\alpha$) (mm^{-1})	20.950	14.432
Crystal size (mm)	$0.20\times0.08\times0.05$	$0.25\times0.04\times0.04$
F(000)	808	1568
Reflections collected	4907	10,710
Independent reflections	1474 ($R_{int}=0.0324$)	1830 ($R_{int}=0.0340$)
Observed data [$I>2\sigma(I)$]	1314	1781
Data/restraints/parameters	1474/0/92	1830/0/91
GOF on F^2	1.098	1.226
R_1, wR_2 ($I>2\sigma(I)$)[a]	0.0223/0.0503	0.0274/0.0482
R_1, wR_2 (all data)	0.0270/0.0521	0.0290/0.0488

[a] $R_1 = \sum||F_o|-|F_c||/\sum|F_o|$,
w$R_2 = \{\sum w[(F_o)^2-(F_c)^2]^2/\sum w[(F_o)^2]^2\}^{1/2}$.

Further details of the crystal structure investigations can be obtained from the Fachinformationszentrum Karlsruhe, 76344 Eggenstein-Leopoldshafen, Germany (Fax: (49) 7247 808 666; e-mail: crysdata@fiz-karlsruhe.de), on quoting the depository numbers CSD 416232 and 416233.

3. Results and discussion

3.1. Structural description for $BaZn(SeO_3)_2$

The structure of $BaZn(SeO_3)_2$ features a three-dimensional (3D) network composed of double chains of $[Zn(SeO_3)_2]^{2-}$ anions bridged by Ba^{2+} cations (Fig. 1). The asymmetric unit of $BaZn(SeO_3)_2$ contains one barium(II), one zinc(II) and two selenite anions. The zinc atom is tetrahedrally coordinated by four selenite oxygen atoms with Zn–O distances ranging from 1.939(4) to 1.988(3) Å. The O–Zn–O bond angles fall in the range of 91.8(1)–118.6(1)°. Both selenium(IV) atoms are three-coordinated by three oxygen atoms in a distorted ψ-SeO_3 trigonal pyramidal geometry with the pyramidal site

Table 2
Atomic coordinates ($\times 10^4$) and displacement parameters ($\times 10^3$ Å^2) for $BaZn(SeO_3)_2$ and $BaZn(TeO_3)Cl_2$

Atom	x	y	z	U_{eq}
$BaZn(SeO_3)_2$				
Ba(1)	1338(1)	2827(1)	6496(1)	12(1)
Zn(1)	1505(1)	789(1)	9065(1)	13(1)
Se(1)	1225(1)	3678(1)	1651(1)	11(1)
Se(2)	8773(1)	9340(1)	6687(1)	12(1)
O(1)	9025(6)	3517(2)	3097(4)	14(1)
O(2)	956(6)	2821(2)	422(5)	19(1)
O(3)	3719(5)	3486(2)	3226(4)	16(1)
O(4)	6926(6)	9110(2)	8341(5)	19(1)
O(5)	9783(7)	8451(2)	6035(5)	22(1)
O(6)	1235(6)	9677(2)	8161(5)	22(1)
$BaZn(TeO_3)Cl_2$				
Ba(1)	3339(1)	2500	3299(1)	16(1)
Ba(2)	5562(1)	7500	2099(1)	17(1)
Zn(1)	5119(1)	7500	4069(1)	14(1)
Zn(2)	5702(1)	2500	731(1)	16(1)
Te(1)	6404(1)	2500	3399(1)	14(1)
Te(2)	7251(1)	7500	471(1)	13(1)
O(1)	6608(4)	2500	2459(2)	26(1)
O(2)	5362(2)	79(6)	3395(2)	19(1)
O(3)	8576(4)	7500	909(3)	33(1)
O(4)	6694(2)	9918(6)	1033(2)	15(1)
Cl(1)	8037(2)	7500	2602(1)	29(1)
Cl(2)	4398(2)	7500	430(1)	32(1)
Cl(3)	4379(1)	2500	1569(1)	23(1)
Cl(4)	6247(2)	7500	4973(1)	45(1)

U_{eq} is defined as one-third of the trace of the orthogonalized U_{ij} tensor.

Table 3
Selected bond lengths (Å) for $BaZn(SeO_3)_2$ and $BaZn(TeO_3)Cl_2$

$BaZn(SeO_3)_2$			
Ba(1)–O(4)#1	2.788(4)	Ba(1)–O(5)#2	2.797(3)
Ba(1)–O(5)#3	2.814(4)	Ba(1)–O(1)#4	2.830(3)
Ba(1)–O(2)#5	2.847(3)	Ba(1)–O(1)#6	2.852(3)
Ba(1)–O(3)#4	2.952(3)	Ba(1)–O(2)#7	2.953(3)
Ba(1)–O(3)	3.020(3)	Ba(1)–O(2)#4	3.174(4)
Ba(1)–O(6)#1	3.321(4)	Zn(1)–O(6)#8	1.939(4)
Zn(1)–O(4)#9	1.966(3)	Zn(1)–O(3)#4	1.985(3)
Zn(1)–O(1)#4	1.988(3)	Se(1)–O(3)	1.662(3)
Se(1)–O(2)	1.712(3)	Se(1)–O(1)	1.714(3)
Se(2)–O(5)	1.652(3)	Se(2)–O(4)	1.700(3)
Se(2)–O(6)	1.720(3)		
$BaZn(TeO_3)Cl_2$			
Ba(1)–O(1)#1	2.585(5)	Ba(1)–O(4)#2	2.810(3)
Ba(1)–O(4)#3	2.810(3)	Ba(1)–O(2)#4	2.853(3)
Ba(1)–O(2)	2.853(3)	Ba(1)–O(3)#1	3.219(3)
Ba(1)–O(3)#2	3.219(3)	Ba(1)–Cl(1)#2	3.331(1)
Ba(1)–Cl(1)#1	3.331(1)	Ba(1)–Cl(4)#5	3.355(2)
Ba(1)–Cl(3)	3.559(2)	Ba(2)–O(4)#6	2.829(3)
Ba(2)–O(4)	2.829(3)	Ba(2)–O(2)#7	2.891(3)
Ba(2)–O(2)#4	2.891(3)	Ba(2)–Cl(1)#1	3.169(2)
Ba(2)–O(1)#7	3.180(2)	Ba(2)–O(1)	3.180(2)
Ba(2)–Cl(1)	3.205(2)	Ba(2)–Cl(3)	3.337(1)
Ba(2)–Cl(3)#7	3.337(1)	Ba(2)–Cl(2)	3.510(2)
Zn(1)–O(3)#1	1.905(5)	Zn(1)–O(2)#4	1.970(3)
Zn(1)–O(2)#7	1.970(3)	Zn(1)–Cl(4)	2.225(2)
Zn(2)–O(4)#6	1.990(3)	Zn(2)–O(4)#8	1.990(3)
Zn(2)–Cl(2)#9	2.232(2)	Zn(2)–Cl(3)	2.291(2)
Te(1)–O(1)	1.821(5)	Te(1)–O(2)	1.877(3)
Te(1)–O(2)#4	1.877(3)	Te(2)–O(3)	1.839(5)
Te(2)–O(4)#6	1.870(3)	Te(2)–O(4)	1.870(3)

Symmetry transformations used to generate equivalent atoms:
For $BaZn(SeO_3)_2$: #1: $-x+1/2$, $y-1/2$, $-z+3/2$; #2: $-x+1$, $-y+1$, $-z+1$; #3: $-x+3/2$, $y-1/2$, $-z+3/2$; #4: $x-1/2$, $-y+1/2$, $z+1/2$; #5: x, y, $z+1$; #6: $x-1$, y, z; #7: $x+1/2$, $-y+1/2$, $z+1/2$; #8: x, $y-1$, z; #9: $-x+1$, $-y+1$, $-z+2$; #10: $x-1/2$, $-y+1/2$, $z-1/2$; #11: $x+1/2$, $-y+1/2$, $z-1/2$; #12: $x+1$, y, z; #13: $-x+3/2$, $y+1/2$, $-z+3/2$; #14: x, y, $z-1$; #15: $-x+1/2$, $y+1/2$, $-z+3/2$; #16: x, $y+1$, z.
For $BaZn(TeO_3)Cl_2$: #1: $x-1/2$, y, $-z+1/2$; #2: $x-1/2$, $y-1$, $-z+1/2$; #3: $x-1/2$, $-y+3/2$, $-z+1/2$; #4: x, $-y+1/2$, z; #5: $-x+1$, $-y+1$, $-z+1$; #6: x, $-y+3/2$, z; #7: x, $y+1$, z; #8: x, $y-1$, z; #9: $-x+1$, $-y+1$, $-z$; #10: $x+1/2$, y, $-z+1/2$; #11: $x+1/2$, $y+1$, $-z+1/2$.

occupied by the lone pair of Se(IV). The Se–O distances fall in the range of 1.651(3)–1.717(4) Å, and O–Se–O bond angles range from 98.2(2)° to 104.6(2)°, which are comparable to those reported in other metal selenites [1,6–10]. Results of bond valence calculations indicate that all selenium atoms are in +4 oxidation state [23]. The calculated total bond valences are 4.15 and 4.19, respectively, for Se(1) and Se(2).

The interconnection of ZnO_4 tetrahedra by bridging selenite groups resulted in a double chain of $[Zn(SeO_3)_2]^{2-}$ (Fig. 2a). Within the double chain, a pair of ZnO_4 tetrahedra is bridged by a pair of $Se(2)O_3$ groups to form a Zn_2Se_2 four-member ring. Neighboring Zn_2Se_2 rings are further bridged by a pair of $Se(1)O_3$ groups into a double chain, resulting in the formation of Zn_4Se_4 eight-member rings. The above two types of rings are alternating along the *a*-axis.

It should be noted that the structure of $BaZn(SeO_3)_2$ is different from those of $SrZn(SeO_3)_2$ [15], $BaCo(SeO_3)_2$ [16], $MCu(SeO_3)_2$ (M = Sr, Ba) [17], $SrMn(SeO_3)_2$ [18], and $SrCu(TeO_3)_2$ [19], although their structural formulae are comparable. Though $SrZn(SeO_3)_2$ crystallizes in a same space group as $BaZn(SeO_3)_2$, its *a*- and *b*-axes are much shortened (~1.05 and 1.67 Å, respectively), whereas its *c*-axis is significantly elongated (2.26 Å); hence, they form two different types of structures. $SrZn(SeO_3)_2$ features a $[Zn(SeO_3)_2]^{2-}$ layer which contains exclusive 16-member ring as a structural building unit (Fig. 2b) [15]. In $BaCo(SeO_3)_2$, the cobalt(II) ion is octahedrally coordinated by six oxygen atoms and these CoO_6 octahedra are bridged by SeO_3 groups into a 3D network of $[Co(SeO_3)_2]^{2-}$ anions, forming tunnels composed of 4 and 12 rings (Fig. 2c) [16]. There are three different structure types for $BaCu(SeO_3)_2$ [17]. Both $BaCu(SeO_3)_2$-I (orthorhombic $Pnm2_1$) and -II (monoclinic $P2_1/c$) contain $[Cu(SeO_3)_2]^{2-}$ sheets formed by CuO_4 squares and SeO_3 groups parallel to the *bc* plane. However, these sheets are topologically different: in $BaCu(SeO_3)_2$-I they are formed by the connection of $Cu_2(SeO_3)$ and $Cu_6(SeO_3)_4$ rings while in $BaCu(SeO_3)_2$-II they are formed by $Cu_2(SeO_3)_2$ and $Cu_6(SeO_3)_6$ rings. The $Cu(SeO_3)_2$ sheets are rugged in $BaCu(SeO_3)_2$-I and they are slightly waved in $BaCu(SeO_3)_2$-II. In both compounds they are connected to each

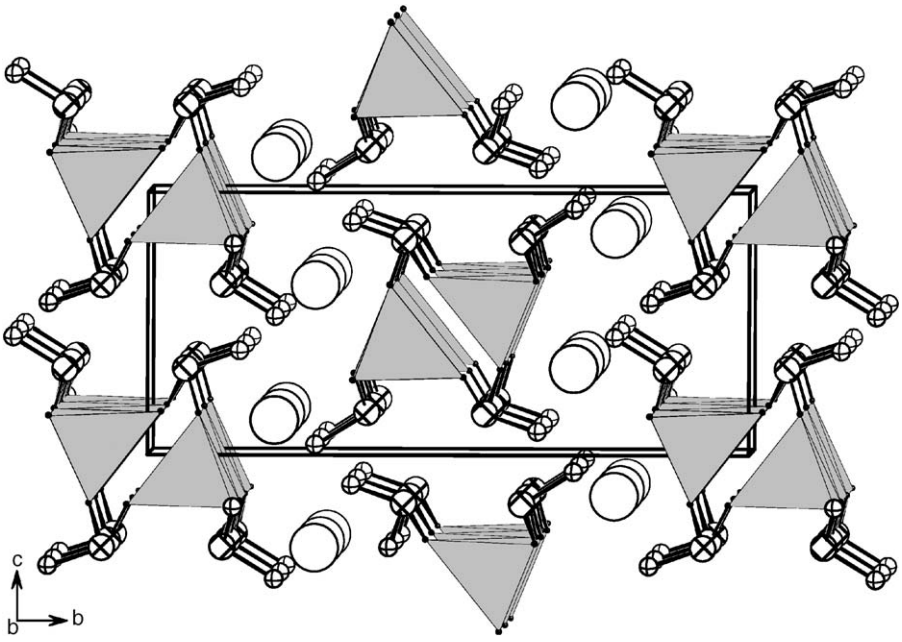

Fig. 1. View of the structure of $BaZn(SeO_3)_2$ down the *a*-axis. ZnO_4 polyhedra are shaded in gray. Ba, Se and O atoms are represented by open (large), hatched and crossed circles, respectively.

other by a fifth Cu–O bond and by the Ba atoms. In $BaCu(SeO_3)_2$-III (monoclinic $C2/c$) and in its isotypic Sr analog, the CuO_4 "squares" and the selenite groups form parallel chains [010], which are connected by the alkaline earth atoms [17].

The charge-balancing barium(II) cations in $BaZn(SeO_3)_2$ are located at the interchain regions and fuse these double chains into a 3D network (Fig. 1). The Ba^{2+} cation has irregular 11-fold coordination by selenite oxygen atoms with the Ba–O distances in the range of 2.788(4)–3.321(4) Å (Table 3).

3.2. Structural description for $BaZn(TeO_3)Cl_2$

$BaZn(TeO_3)Cl_2$ is a new mixed metal Te(IV) oxychloride. Its structure features a 3D network in which double chains of $[Zn_2(TeO_3)_2Cl_3]^{3-}$ anions are separated by barium(II) ions and chloride anions (Fig. 3). Both zinc(II) ions in the asymmetric unit are in a tetrahedral environment. Zn(1) is coordinated by three tellurite oxygens and a chloride anion, whereas Zn(2) is coordinated by two chloride anions and two tellurite oxygens. The Zn–Cl distances (2.225(2)–2.291(2) Å) are significantly longer than those of the Zn–O bonds (1.905(3)–1.990(3) Å). These Zn–O and Zn–Cl distances are comparable to those reported in $Zn_2(TeO_3)Cl_2$ [13]. Both Te(1) and Te(2) are in a distorted Ψ-TeO_3 trigonal pyramidal geometry with the pyramidal site occupied by the lone pair electrons of Te(IV) (Fig. 4). The Te–O distances are in the range of 1.821(5)–1.877(3) Å. Based on bond valence calculations, both tellurium atoms have an oxidation state of +4, the calculated total bond valences are 4.14 and 4.12 for Te(1) and Te(2), respectively [23].

It is interesting to note that $Zn(2)O_2Cl_2$ tetrahedra and $Te(2)O_3$ groups are interconnected via corner-sharing O(4) atoms to form a chain along the *b*-axis. Likewise, $Zn(1)O_3Cl$ tetrahedral and $Te(1)O_3$ groups are also interconnected via corner-sharing O(2) atoms to form a chain along the *b*-axis. The above two chains are interlocked into a double chain of $[Zn_2(TeO_3)_2Cl_3]^{3-}$ via Te(2)–O(3)–Zn(1) bridges (Fig. 4), resulting in the formation of Zn_3Te_3 six-member rings. $Te(1)O_3$ groups share two corners with zinc tetrahedra, whereas $Te(2)O_3$ group connects with three zinc(II) centers. It is worthy to note that $Zn_2(TeO_3)Cl_2$ has a layered structure in which ZnO_4Cl square pyramids, ZnO_2Cl_2 tetrahedra and tellurite anions are interconnected via corner and edge sharing [13].

Ba(1) is 11-coordinated by seven tellurite oxygens and four chloride anions, whereas Ba(2) is 11-coordinated by six tellurite oxygens and five chloride anions. The Ba–O and Ba–Cl distances are comparable to those reported in $Ba_3(TeO_3)_2Cl_2$ [24]. The interconnection of barium(II) ions by bridging Cl(1) and Cl(3) anions leads to a (400) $[Ba_2Cl_2]^{2+}$ layer (Fig. 5). Cl(1) and Cl(3) connect with four and two Ba^{2+} cations, respectively. The above double chains of $[Zn_2(TeO_3)_2Cl_3]^{3-}$ and 2D barium chloride layers are further interconnected via Ba–Cl–Zn and Ba–O–Te bridges, resulting in a complex 3D network structure with long-narrow shaped tunnels running along the *b*-axis (Fig. 3). The lone pair electrons of the Te(IV) ions are oriented toward the above tunnels.

It is interesting to compare the double chain of $[Zn_2(TeO_3)_2Cl_3]^{3-}$ in $BaZn(TeO_3)Cl_2$ with that of $[Zn(SeO_3)_2]^{2-}$ anions in $BaZn(SeO_3)_2$. All zinc(II) ions are in tetrahedral geometry. Each tellurite group in $BaZn(TeO_3)Cl_2$ connects with three zinc(II) ions, whereas

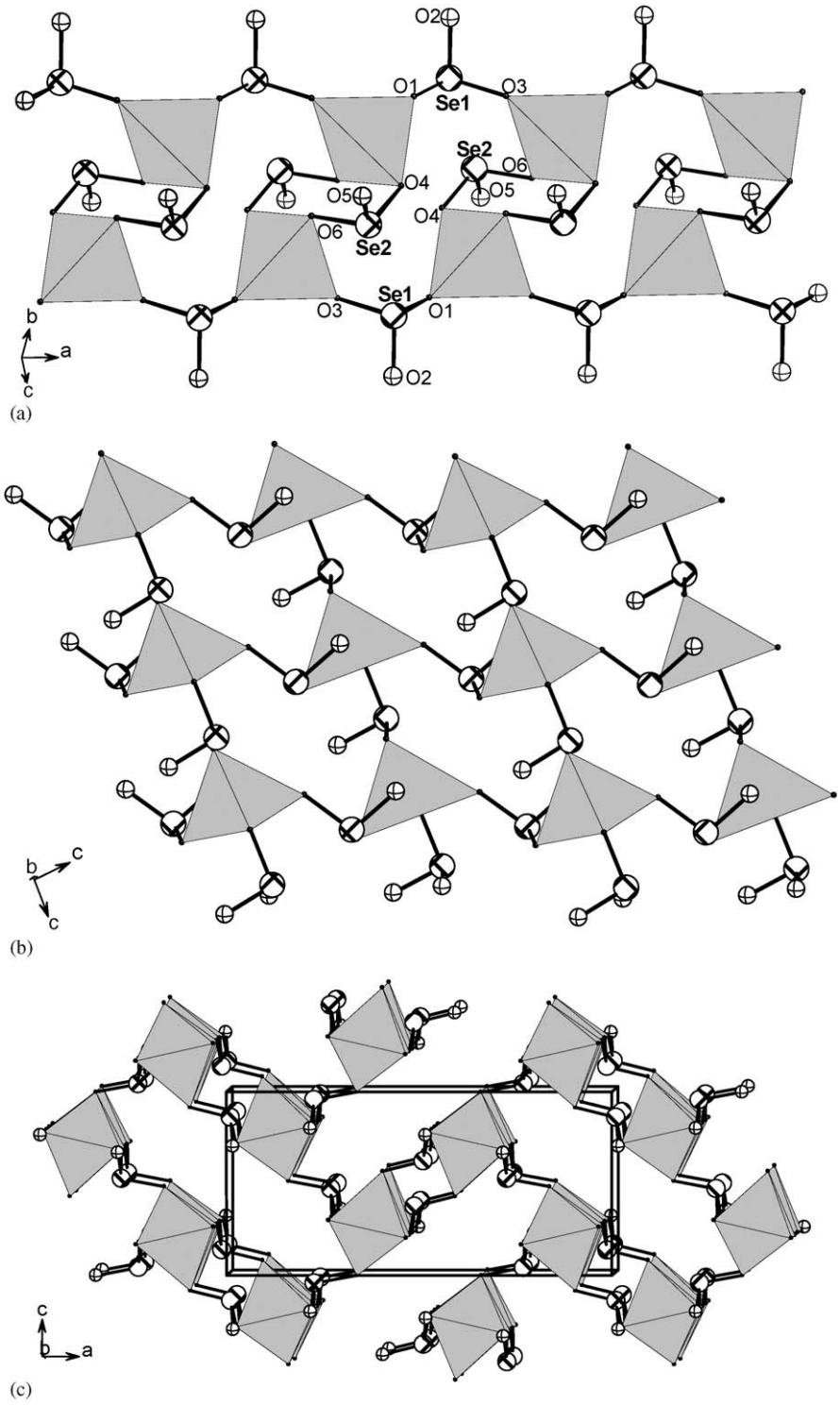

Fig. 2. Comparison of 1D double chain of $[Zn(SeO_3)]^{2-}$ along *a*-axis in $BaZn(SeO_3)_2$ (a) with layered $[Zn(SeO_3)_2]^{2-}$ in $SrZn(SeO_3)_2$ (b) and 3D $[Co(SeO_3)_2]^{2-}$ in $BaCo(SeO_3)_2$. ZnO_4 polyheda or CoO_6 octahedra are shaded in gray. Se and O atoms are represented by hatched and crossed circles, respectively.

each selenite group bonds to only two zinc(II) ions. Due to the coordination of some chloride anions with zinc(II) ions, the double chain structure of $[Zn_2(TeO_3)_2Cl_3]^{3-}$ is much simpler than that of $[Zn(SeO_3)_2]^{2-}$ anions in $BaZn(SeO_3)_2$. $[Zn_2(TeO_3)_2Cl_3]^{3-}$ contains only Zn_3Te_3 six-member rings, whereas $[Zn(SeO_3)_2]^{2-}$ is composed of Zn_2Se_2 and Zn_4Se_4 rings.

The observed XRD powder patterns for $BaZn(SeO_3)_2$ and $BaZn(TeO_3)Cl_2$ match well with those simulated from single crystal structure data (see Supporting Materials),

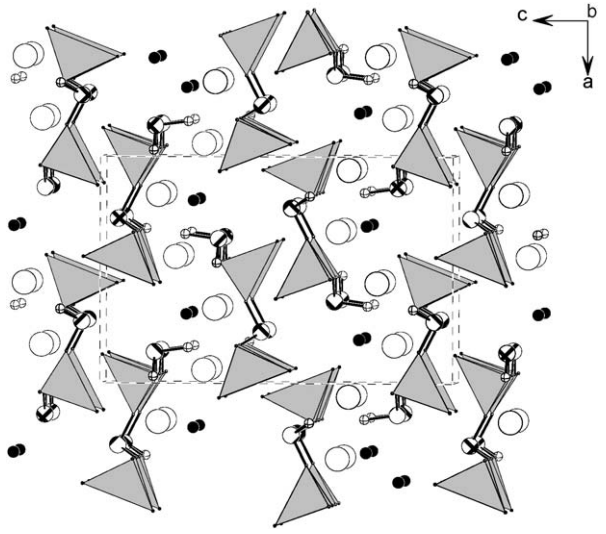

Fig. 3. View of the structure of $BaZn(TeO_3)Cl_2$ down the *b*-axis. ZnO_3Cl and ZnO_2Cl_2 tetrahedra are shaded in gray. Ba, Te, Cl and O atoms are represented by open (large), hatched, black and crossed circles, respectively.

indicating that both compounds were isolated as single phases.

3.3. IR, TGA and optical properties for $BaZn(SeO_3)_2$ and $BaZn(TeO_3)Cl_2$

IR studies indicate that $BaZn(SeO_3)_2$ and $BaZn(TeO_3)Cl_2$ are transparent in the range of 4000–1000 cm^{-1}. The absorption bands of $BaZn(SeO_3)_2$ at 854, 799 and 720 cm^{-1} can be assigned to ν(Se–O) vibrations, whereas those at 596, 499, 459 and 421 cm^{-1} are originated from ν(O–Se–O) vibrations. The absorption bands of $BaZn(TeO_3)Cl_2$ at 738 and 687 cm^{-1} are characteristic of ν(Te–O) vibrations, absorption bands at 574 and 471 cm^{-1} can be assigned to $\nu(M$–O) vibrations, and band at 418 cm^{-1} is originated from ν(Te–O–*M*) vibrations. All of the assignments are consistent with those previously reported [25].

TGA indicate that $BaZn(SeO_3)_2$ is stable up to 435 °C (see Supporting Materials). The weight loss occurred in the range of 435–721 °C corresponding to the release of one

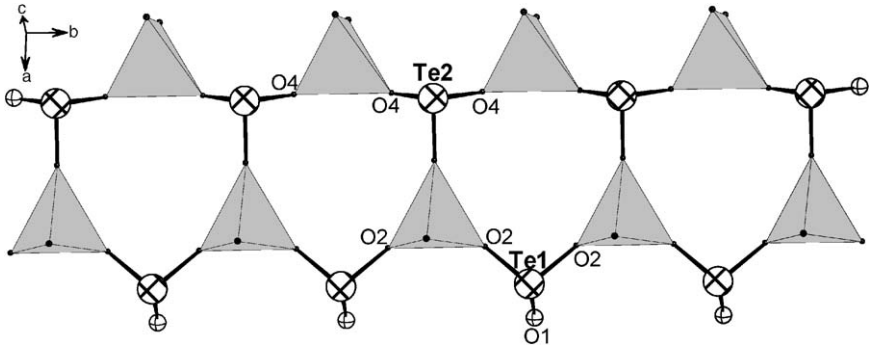

Fig. 4. A 1D double chain of $[Zn_2(TeO_3)_2Cl_3]^{3-}$ along *b*-axis. ZnO_3Cl and ZnO_2Cl_2 tetrahedra are shaded in gray. Te and O atoms are represented by hatched and crossed circles, respectively.

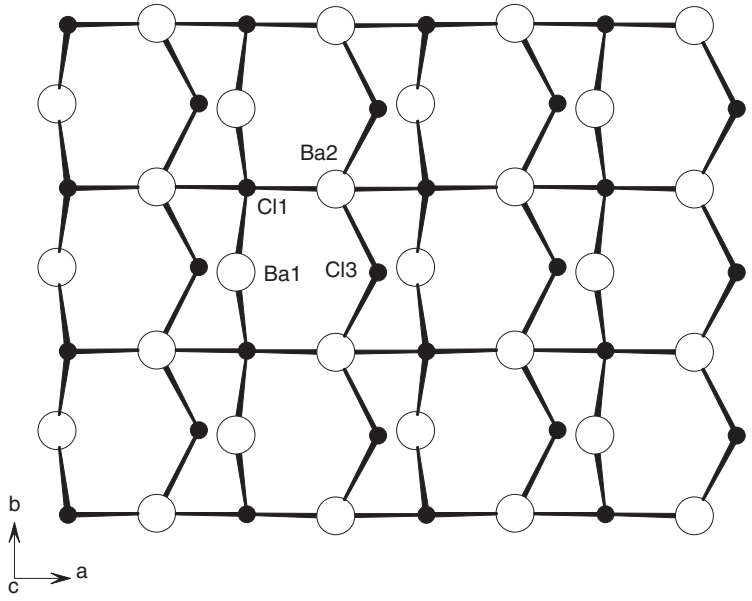

Fig. 5. A 2D barium chloride layer perpendicular to *c*-axis.

SeO_2. The observed weight loss of 25.3% is close to the calculated value (24.3%). $BaZn(TeO_3)Cl_2$ is stable up to about 600 °C. Then it decomposes continuously up to 1200 °C, during which TeO_2 and Cl_2 are released. The observed total weight loss is 46.9% and final residue is not characterized.

Optical diffuse reflectance spectra of the two compounds reveal optical band gaps of 3.8 and 4.4 eV, respectively, for $BaZn(SeO_3)_2$ and $BaZn(TeO_3)Cl_2$ (see Supporting Information). Hence, both the compounds are wide bandgap semiconductors.

Acknowledgments

The authors gratefully acknowledge the support from the National Natural Science Foundation of China (Nos. 20573113, 20371047 and 20521101) and NSF of Fujian Province (No. E0420003).

Appendix A. Supporting Information

Supplementary data associated with this article can be found in the online version at doi:10.1016/j.jssc.2006.03.018.

References

[1] (a) M.S. Wickleder, Chem. Rev. 102 (2002) 2011 (and references therein);
(b) V.P. Verma, Thermochim. Acta 327 (1999) 63 (and references therein).
[2] (a) H.-S. Ra, K.-M. Ok, P.S. Halasyamani, J. Am. Chem. Soc. 125 (2003) 7764;
(b) K.-M. Ok, P.S. Halasyamani, Inorg. Chem. 43 (2004) 4248;
(c) K.-M. Ok, J. Orzechowski, P.S. Halasyamani, Inorg. Chem. 43 (2004) 964;
(d) J. Goodey, K.-M. Ok, J. Broussard, C. Hofmann, F.V. Escobedo, P.S. Halasyamani, J. Solid State Chem. 175 (2003) 3.
[3] (a) R.T. Hart, K.-M. Ok, P.S. Halasyamani, J.W. Zwanziger, Appl. Phys. Lett. 85 (2004) 938;
(b) Y. Porter, P.S. Halasyamani, J. Solid State Chem. 174 (2003) 441;
(c) J. Goodey, J. Broussard, P.S. Halasyamani, Chem. Mater. 14 (2002) 3174;
(d) K.-M. Ok, P.S. Halasyamani, Chem. Mater. 13 (2001) 4278.
[4] (a) W.T.A. Harrison, L.L. Dussack, A.J. Jacobson, J. Solid State Chem. 125 (1996) 234;
(b) V. Balraj, K. Vidyasagar, Inorg. Chem. 38 (1999) 5809;
(c) V. Balraj, K. Vidyasagar, Inorg. Chem. 38 (1999) 3458.
[5] (a) R. Becker, M. Johnsson, R. Kremer, P. Lemmens, Solid State Sci. 5 (2003) 1411;
(b) M. Johnsson, K.W. Törnroos, F. Mila, P. Millet, Chem. Mater. 12 (2000) 2853;
(c) M. Johnsson, K.W. Törnroos, P. Lemmens, P. Millet, Chem. Mater. 15 (2003) 68;
(d) M. Johnsson, S. Lidin, K.W. Törnroos, H.-B. Bűrgi, P. Millet, Angew. Chem. Int. Ed. 43 (2004) 4292.
[6] (a) K. Kohn, K. Inoue, O. Horie, S. Akimoto, J. Solid State Chem. 18 (1976) 27;
(b) R. Escamilla, A.J.M. Gallardo, E. Moran, M.A. Alario-Franco, J. Solid State Chem. 168 (2002) 149;
(c) W. Bensch, J.R. Guenther, Z. Kristallogr. 174 (1986) 291;
(d) F.C. Hawthorne, T.S. Ercit, L.A. Groat, Acta Crystallogr. C 42 (1986) 1285.
[7] G. Meunier, M. Bertaud, Acta Crystallogr. B 30 (1974) 2840.
[8] T.F. Semenova, I.V. Rozhdestvenskaya, S.K. Filatov, L.P. Vergasova, Mineral. Mag. 56 (1992) 241.
[9] G. Giester, Acta Chem. Scand. 49 (1995) 824.
[10] G. Giester, Monatsh. Chem. 127 (1996) 347.
[11] K. Hanke, Naturwissenschaften 54 (1967) 199.
[12] (a) C.R. Feger, G.L. Schimek, J.W. Kolis, J. Solid State Chem. 143 (1999) 246;
(b) K. Hanke, Naturwissenschaften 53 (1966) 273.
[13] M. Johnsson, K.W. Törnroos, Acta Crystallogr. C 59 (2003) i53.
[14] M. Johnsson, K.W. Törnroos, Solid State Sci. 5 (2003) 263.
[15] M.G. Johnston, W.T.A. Harrison, Inorg. Chem. 40 (2001) 6518.
[16] G. Giester, M. Wildner, J. Alloy Compd. 239 (1996) 99.
[17] H. Effenberger, J. Solid State Chem. 70 (1987) 303.
[18] M.G. Johnston, W.T.A. Harrison, Acta Crystallogr. C 58 (2002) 33.
[19] H. Mueller-Buschbaum, L. Wulff, Z. Naturforsch. B 52 (1997) 1341.
[20] W.M. Wendlandt, H.G. Hecht, Reflectance Spectroscopy, Interscience, New York, 1966.
[21] CrystalClear ver. 1.3.5., Rigaku Corp., Woodlands, TX, 1999.
[22] G.M. Sheldrick, SHELXTL, Crysytallographyic Software Package, SHELXTL, Version 5.1, Bruker-AXS, Madison, WI, 1998.
[23] I.D. Brown, D. Altermat, Acta Crystallogr. B 41 (1985) 244.
[24] D. Hottentot, B.O. Loopstra, Acta Crystallogr. C 39 (1983) 1600.
[25] (a) Y.-L. Shen, J.-G. Mao, J. Alloy Compd. 385 (2004) 86;
(b) M.-L. Feng, J.-G. Mao, J. Alloy Compd. 388 (2005) 23;
(c) Y. Porter, P.S. Halasyamani, Inorg. Chem. 42 (2003) 205.